Estimation of the Ischemic Penumbra Based on CT Perfusion:

A Pilot Study

Zhihua Sun, PhD, Xuejun Zhang, MS, Yunting Zhang, PhD, Hong Guo, En, Jing Zhang, PhD, Chunshui Yu, PhD

Rationale and Objectives: Ischemic penumbra (IP), the target of thrombolytic therapies, could be estimated by the mismatch region between magnetic resonance imaging (MRI) diffusion- and perfusion-defined abnormalities; however, the accuracy of this method has been challenged recently. In this study, we try to establish a method for calculating IP size based on computed tomography perfusion (CTP) and to observe the early evolution of IP in detail.

Materials and Methods: The middle cerebral artery occlusion (MCAO) model in monkey was used to compare the accuracy in estimating the IP between CTP and MRI methods. A receiver operating characteristic (ROC) curve was performed to calculate the IP threshold of the different CTP parameters, and then the best parameter was obtained. The dynamic evolutions of estimated size of IP by these two methods were compared.

Results: Among the three CTP parameters, relative cerebral blood flow (rCBF) had the highest sensitivity (83.3%) and specificity (98.5%) in estimating the IP. The optimal cutoff threshold of rCBF was 0.203. During the first 15 hours of the MCAO model, the estimated size of IP by the rCBF was larger than that of the MRI method; however, this relationship was reversed 15 hours later.

Conclusion: This study suggests that the rCBF method is more accurate in estimating the IP since previous studies have reported that the MRI method underestimated the exact IP in the early stage of ischemia and overestimated the exact IP in the later stages. Further experimental and clinical studies are needed to validate the conclusion.

Key Words: Computed tomography perfusion; magnetic resonance imaging; receiver operating characteristic curve; ischemic penumbra; brain.

©AUR, 2010

In the field of ischemic stroke, ischemic penumbra (IP) is an important concept, proposed by Astrup in 1981 (1). It refers to the regions of brain tissue, usually peripheral in location, where blood flow is sufficiently reduced to cause hypoxia, severe enough to arrest physiological function, but not so complete as to cause irreversible failure of energy metabolism and cellular necrosis (2,3). IP is the target for thrombolytic therapy, which remains the only approved therapy for acute ischemic stroke. The existence time of the IP largely varied individually. So accurately estimating the size of IP is one of the important factors for deciding whether the thrombolytic therapy is needed or not, optimizing the therapeutic methods of ischemic stroke, monitoring the evolution of the disease, and assessing the outcome of the therapy.

Acad Radiol 2010; 17:1535–1542

From the Department of Radiology (Z.S., X.Z., Y.Z., H.G., J.Z., C.Y.), Tianjin Medical University General Hospital, No. 154, Anshan Dao Road, Heping District, Tianjin, the People's Republic of China, 300052. Received May 4, 2010; accepted August 3, 2010. Supported by the National Nature Science Funds (30370434) and National Basic Research Program of China (973 Program, 2010CB732500). **Address correspondence to:** Y.Z. e-mail: cjr.zhangyunting@vip.163.com

©AUR, 2010
doi:10.1016/j.acra.2010.08.016

Positron emission tomography (PET) can combine perfusion and metabolism information, and is regarded as the gold standard in estimating the IP with reduced cerebral blood flow (CBF) but preserved cerebral metabolic rate for oxygen and raised oxygen extraction fraction (4,5). However, PET is not suitable for assessing hyperacute and acute infarcts because it is expensive, radioactive, and not available in some clinical settings.

Magnetic resonance imaging (MRI) is the most widely used technique for assessment of IP (6). The MRI method is based on a perfusion-diffusion mismatch model, in which the IP is calculated by the perfusion-deficit volume minus the diffusion-abnormal volume (7,8). In this model, the lesion on diffusion-weighted imaging (DWI) is thought to approximate the irreversibly damaged brain tissue. However, reversible DWI lesions have been reported, particularly after thrombolysis (9–13). Specifically, Desmond et al (9) and Liu et al (10) reported that the brain tissue with apparent diffusion coefficient, decreased to 40%–60% of normal tissue, represented irreversible infarction, whereas the tissue with apparent diffusion coefficient decreased to 75%–90% represented IP. Moreover, several authors have demonstrated that diffusion lesions may be partially or even fully reversible when reperfusion occurs within 2–3 hours and in as many as 20% of patients

in the 6-hour time window (12,13). Similarly, the low perfusion regions around the infarct core on perfusion-weighted imaging (PWI) cannot be fully categorized as IP because parts of the regions were benign oligemia (14). Hence, the mismatch between PWI and DWI could be much larger than the true IP, especially at the early stage of stroke.

The computed tomography (CT) has widespread availability, short examination time, and high cost-effectiveness, and can exclude hemorrhagic lesions at an early stage. CT perfusion (CTP) can approximately estimate the IP region characterized by lower CBF but normal or higher cerebral blood volume (CBV) (15–17). The infarct core is roughly defined as the region with CBV < 2 mL/100 g, and the IP is considered as the surrounding regions with decreased CBF and increased mean transit time (MTT), compared to the corresponding contralateral brain tissue >145% (18,19). However, the available quantitative method for estimating the IP is relatively rare. Moreover, most of the human stroke studies can not observe the early evolution of IP in very short intervals (such as 1–2 hours).

The purpose of our study is to establish a CTP method to estimate the IP size using receiver operating characteristic (ROC) analysis, to observe the early evolution of IP in detail, and to compare the accuracy of this method with the MRI method.

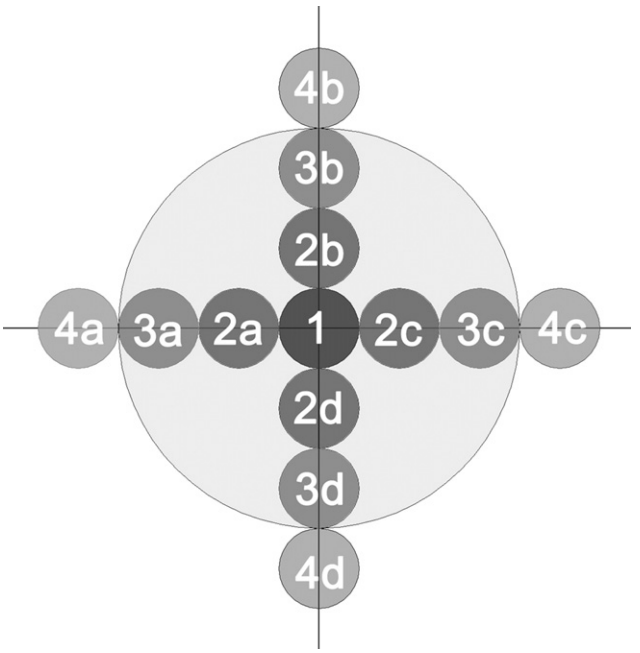

Figure 1. Selection of four regions of interest (ROIs) in ischemic region of monkey middle cerebral artery occlusion model. Yellow region represents the infarct region on T_2-weighted imaging (T2WI) at 24 hours. ROIs 1, 2, and 3 were located within the infarct region, but ROI 4 was in the peripheral region adjacent to the infarct region.

MATERIALS AND METHODS

Animal Model

The experiment was approved by Animal Care and Use Committee of Tianjin Medical University. Seven male monkeys (Macaca Mulatta) with a mean age of 6.2 years (range 5–7 years) and a mean weight of 7.3 kg (range 6–8 kg) were supplied by Experimental Animal Center of Beijing Military Medical Academy. The middle cerebral artery occlusion (MCAO) model was established by an autothrombus interventional method. After a selected monkey was anaesthetized and disinfected, the right femoral artery was separated and punctured, and then the 5F catheter sheath and the 4F catheter were placed in. One side of the middle cerebral artery that is more suitable for the autothrombus interventional method was chosen according to the bilateral vertebral and internal carotid arteries angiography. Then a 3F-SP catheter was induced to the artery through the 4F catheter, and positioned in the middle cerebral artery. We pulled and rotated the 3F-SP catheter to induce thrombosis. Finally, we pulled out the catheter and ligated the right femoral artery after 20–30 minutes. The monkeys maintained an anaesthetized state during MRI and CT examinations.

CT and MRI Examination

CTP, MR DWI, and PWI were performed at 1 hour, 5 hours, 10 hours, 15 hours, 20 hours, and 24 hours after MCAO consecutively. To maintain the consistency of slices on CT and MRI, the same slice thickness and field of view (FOV) were used, and the first slice was fixed on the line between the nose point and the midpoint of sellae. The CTP examination was performed with a GE LightSpeed pro 16 CT scanner. We started scanning before 20 mL iohexol (370 mgI/mL) was injected at 2 mL/second. A total of 792 slices were obtained, with a slice thickness of 2.5mm, FOV of 18 cm × 18 cm, tube voltage of 80 KV, and tube current of 100 mA.

MRI was performed with a GE 1.5T Twin Speed Infinity with Excite I magnetic resonance system. DWI, PWI and T_2-weighted imaging (T_2WI) were performed with a head coil. T_2WI parameters included: repetition time (TR) = 4000 ms; echo time (TE) = 106.4 ms; average = 2; slice thickness = 2.5 mm; gap = 0 mm, FOV = 18 cm × 18 cm, matrix = 288 × 256. DWI was obtained using a single shot spin-echo echo planar sequence, with TR = 6000 ms; TE = 96.8 ms; average = 2; b = 1000s/mm^2; FOV = 18 cm × 18 cm, matrix = 128 × 128. PWI was obtained using a single shot gradient recalled echo planar imaging T_2*WI sequence (ie, dynamic susceptibility contrast MRI), with TR = 2000 ms; TE = 80 ms; averages = 1; FOV = 18 cm × 18 cm, matrix 128 × 128. A Gd-DTPA bolus (0.1 mmol/kg) was administered by power injector at a rate of 2 mL/s, and then 10 mL of isotonic saline was injected to wash the pipe. A total of 330 slices were acquired.

Data Analysis

The parameters of CTP including CBF, CBV, permeability surface (PS), and MTT were processed and measured by perfusion software using a GE Sun AW4.2 work station. To simplify the analysis, we chose the slice through the lateral

TABLE 1. ANOVA among the CTP Parameters of ROIs 1, 2, and 3 within Infarct Lesions in the Monkey MCAO Model (*P* Value)

	rCBF			rCBV			rMTT			PS		
Time point (hours)	1&2	2&3	1&3	1&2	2&3	1&3	1&2	2&3	1&3	1&2	2&3	1&3
1	0.001*	0.003*	0.003*	0.063	0.076	0.008*	0.069	0.566	0.356	0.356	0.256	0.245
5	0.078	0.001*	0.005*	0.111	0.001*	0.001*	0.134	0.145	0.346	0.001*	0.058	0.001*
10	0.135	0.001*	0.0003*	0.456	0.005*	0.003*	0.342	0.466	0.234	0.134	0.005*	0.003*
15	0.222	0.005*	0.005*	0.365	0.005*	0.001*	0.125	0.263	0.464	0.235	0.567	0.450
20	0.141	0.002*	0.001*	0.654	0.564	0.396	0.268	0.295	0.235	0.432	0.452	0.267
24	0.071	0.321	0.235	0.098	0.287	0.345	0.256	0.007*	0.005*	0.535	0.244	0.457

ANOVA, analysis of variance; CTP, computed tomography perfusion; MCAO, middle cerebral artery occlusion; rCBF, relative cerebral blood flow; rCBV, relative cerebral volume; rMTT, relative mean transit time; PS, permeability surface; ROI, region of interest.
*$P < .05$.

ventricle body as the slice of interest, and then all the following analyses were performed on this slice. The final infarct lesion was defined as the T2WI lesion on the slice at 24 hours. After projecting the region of final infarct to each of the CBV, CBF, and MTT maps, we drew two orthogonal lines through the center of the infarct, and marked four series of regions of interest (ROIs) from the center on the two lines (Fig 1). ROIs 1–3 were located within the high signal intensity region on T2WI. ROI 1 was located in the center of the infarct, ROI 3 located in the margin of the infarct, and ROI 2 was between the ROI 1 and ROI 3. ROI 4 demonstrated normal signal intensity on T2WI just adjacent to the region with high signal intensity. The size of ROIs were the same for an individual, but variable among different individuals (range 20–40 mm^2).

The relative ratios between the infarct lesions and contralateral normal brain were calculated, including relative CBV (rCBV), relative CBF (rCBF), and relative MTT (rMTT). Because PS of contralateral normal brain was zero or near to zero, we only measured the absolute PS values of ischemic region. And the ROIs of normal brain were selected at the mirror region relative to the ROIs of ischemic regions. We measured the abnormal signal intensity area of the different parameter maps at each time point and averaged the values of the four series of ROIs 2, 3, and 4.

Statistical Analysis

Statistical analysis was performed with the SPSS 11.0 software package. Differences were considered statistically significant at $P < .05$. Repeated measures variance analysis was used to analyze the difference between four series of ROIs 2, 3, and 4. One-way analysis of variance (ANOVA) was performed among each parameter of ROI 1 and the mean of ROIs 2, 3, and 4. A ROC curve was applied to calculate the IP threshold of the different parameters.

Visualization of IPs

The infarct lesion and IP were visualized based on the optimal IP threshold of the CTP parameter selected from ROC analysis. First, we identified the actual infarct size on T_2WI at 24 hours and copied this region to the gray-level CTP parameter map. Then, we input the IP threshold of the CTP parameter and the pixels with higher value than the threshold would be marked as a red color; then, the proportion of the red region to infarct would be calculated.

RESULTS

Five of the seven monkey MCAO models were performed successfully, including three right and two left sides.

Differences in CTP Parameters between the Four Series of ROI

Repeated measures variance analysis was used to test the possible differences in CTP parameters among the four series of ROI, including ROI 2a, 2b, 2c, and 2d; ROI 3a, 3b, 3c, and 3d; and ROI 4a, 4b, 4c, and 4d. There were no statistical differences in rCBF, rCBV, rMTT, and PS among different ROIs 2, 3. and 4 ($P > .05$). So we used the means of ROIs 2, 3, and 4 to perform ANOVA and ROC analysis.

Differences in CTP parameters between ROIs at different time points

One-way ANOVA was performed among the CTP parameters of ROIs 1, 2, and 3 at each time point (Table 1). For correcting for multiple comparisons, Bonferroni method was used. There were significant differences in rCBF between ROIs 1 and 2, 2 and 3, 1 and 3 at 1 hour, between ROIs 2 and 3, 1 and 3 from 5 hours to 20 hours ($P < .05$), whereas there were no significant differences among ROIs 1, 2, and 3 at 24 hours ($P > .05$). There were significant differences in rCBV between ROIs 1 and 3 at 1 hour, between ROIs 2 and 3, 1 and 3 from 5 hours to 15 hours ($P < .05$), whereas no significant differences among ROIs 1, 2, and 3 at 20 and 24 hours ($P > .05$). There were significant differences in rMTT between ROIs 2 and 3, 1 and 3 only at 24 hours ($P < .05$), whereas there were no significant differences among ROIs 1, 2, and 3 from 1 hour to 20 hours ($P > .05$). There were significant differences in PS between ROIs 1 and 2, 1 and 3 only at 5 hours, between ROIs 2 and 3, 1 and 3 at 10

TABLE 2. ROC Curve Analysis of the CTP Parameters

Parameter	Area under the Curve ($\bar{x} \pm s$)	*P*	Threshold	Sensitivity	Specificity
rCBF	0.971 ± 0.015	<.001	0.203	83.3%	98.5%
rCBV	0.924 ± 0.028	<.001	0.483	79.2%	86.4%
rMTT	0.436 ± 0.066	.352	(—)	(—)	(—)
PS	0.498 ± 0.079	.330	(—)	(—)	(—)

See Table 1 for abbreviations.
The diagnostic effect would be better if the area under curve was closer to 1.

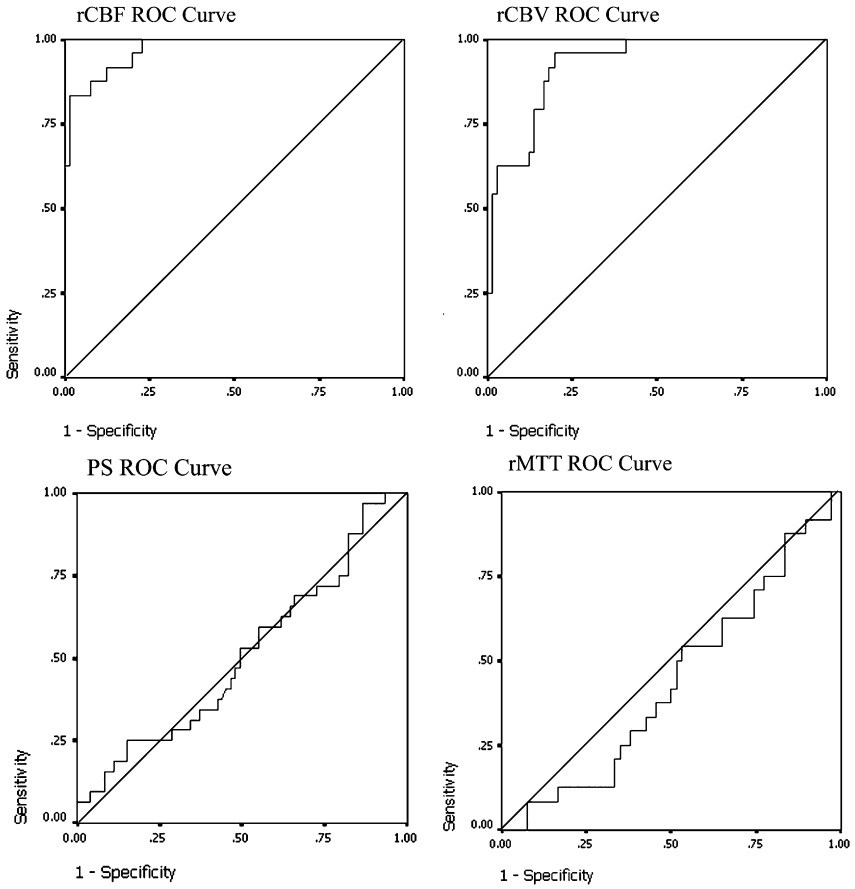

Figure 2. Receiver operating characteristic (ROC) curve analysis of the computed tomography perfusion parameters. rCBF, relative cerebral blood flow; rCBV, relative cerebral volume; rMTT, relative mean transit time; PS, permeability surface.

hours ($P < .05$), whereas there were no significant differences among ROIs 1, 2, and 3 at 1 hour and from 15 to 24 hours ($P > .05$). There were significant differences between the rCBV, rCBF, rMTT, and PS of ROI 4 and those of ROIs 1, 2, and 3 within 24 hours ($P < .05$).

Calculation of IP Thresholds

We calculated the IP thresholds of each parameter by ROC curve (Table 2, Fig 2). The areas under the curves of rCBF and rCBV reached statistical significance ($P < .05$), and the IP thresholds, sensitivity, and specificity of these two parameters were calculated. However, the area under the curve of rMTT and PS had no significance ($P > .05$) and the IP threshold of rMTT and PS could not be calculated. The sensitivity (83.3%) and specificity (98.5%) of rCBF thresholds were higher than those of rCBV threshold (79.2% and 86.4%, respectively).

Changes of Sizes of Ischemic Regions on Different Parameter Maps at Different Time Points

Considering the individual differences in the size of the infarct, the sizes of ischemic lesions in different parameter maps were calculated and standardized by the infarct size on T_2WI at 24 hours. Table 3 shows the ischemic size ratios of the different parameter maps, suggesting that the ischemic region grew progressively in all the parameter maps except for the MTT map. Negative enhance integral (NEI) of PWI was corresponding to CBV of CTP.

TABLE 3. The Ischemic Size Ratios of Imaging Parameters in Monkey MCAO Model ($\bar{x} \pm s$)

Time point (hours)	CBF	CBV	MTT	PS	PWI	DWI
1	0.648 ± 0.203	0.414 ± 0.105	1.023 ± 0.237	1.121 ± 0.119	0.409 ± 0.039	0.831 ± 0.067
5	0.842 ± 0.153	0.491 ± 0.086	1.095 ± 0.218	1.019 ± 0.208	0.487 ± 0.096	0.918 ± 0.132
10	0.956 ± 0.160	0.722 ± 0.145	1.055 ± 0.223	1.238 ± 0.369	0.731 ± 0.175	0.930 ± 0.123
15	1.096 ± 0.249	0.773 ± 0.147	1.113 ± 0.138	1.209 ± 0.321	0.800 ± 0.179	0.963 ± 0.125
20	1.034 ± 0.198	0.774 ± 0.068	1.155 ± 0.141	1.110 ± 0.178	0.818 ± 0.129	1.016 ± 0.083
24	1.109 ± 0.057	0.830 ± 0.076	1.176 ± 0.080	0.998 ± 0.101	0.805 ± 0.123	0.993 ± 0.032

CBF, cerebral blood flow; CBV, cerebral volume; MTT, mean transit time; PS, permeability surface; PWI, perfusion-weighted imaging; DWI, diffusion-weighted imaging.

The ischemic size ratios of imaging parameters are standardized by the infarct size on T_2-weighted imaging at 24 hours.

At 1 and 5 hours after stroke, CTP-MTT ≈ CTP-PS > MR-T2WI > MR-DWI > CTP-CBF > CTP-CBV ≈ MR-PWI(NEI); at 10 hours, CTP-MTT ≈ CTP-PS > MR-T2WI > CTP-CBF > MR-DWI > CTP-CBV ≈ MR-PWI(NEI); from 15 hours to 24 hours, CTP-MTT ≈ CTP-PS > CTP-CBF > MR-T2WI ≈ MR-DWI > CTP-CBV ≈ MR-PWI(NEI).

Evolution of IP Size Estimated by CTP and MRI Methods

Figure 3 shows the evolution of IP in No. 1 monkey. The IP sizes calculated by CTP and MRI methods were listed in Table 4. We found that the IP size calculated by MRI method was lower than that by CTP method before 15 hours and larger at 20 hours and 24 hours (Fig 4). The results by the two methods had statistical difference by paired-samples *t*-test ($t = -3.499$, $P = .002$), and had correlations with each other by correlative analysis ($r = 0.803$, $P < .001$).

DISCUSSION

In ischemic stroke, a compromised blood supply leads to functional impairment, followed by structural disintegration of neurons in the absence of reperfusion. The initial phase of dysfunction is potentially reversible, and the degree of ischemia decreases with distance from the infarct core. Some tissue may be irreversibly damaged and the other hypoperfused regions may be at risk but are potentially salvageable (ie, the IP), which is the target of the thrombolytic therapies (20–22).

In our monkey model, there are significant differences between the CBV and CBF with ROIs 1, 2, and 3 within 15–20 hours, which indicates that the IP of monkey brain may be present until 15–20 hours. However, in human beings, the therapy time limitation for ischemic stroke was 3–6 hours (23). For example, the therapy time window of the retissue-type plasminogen activator was identified as 3 hours by the National Health Association in America (22). In some other clinical series of recanalization and neuroprotective additive drugs, it was below 6 hours (24). But the IP in many patients persists outside this narrow time window. Up to 44% of stroke patients may have penumbral tissue after 18 hours (25). Therefore, estimation of the IP may be relevant in selecting patients who present beyond the 3-hour time window for thrombolytic therapy.

Although reperfusion of the ischemic brain through the recanalization of occluded arteries could salvage reversible ischemic cells and was the most effective therapy for hyperacute and acute infarction, reperfusion could also contribute to brain damage through the mechanism of reperfusion injury. Reperfusion injury has been defined in numerous ways, including activation of the endothelium, excess production of oxygen free radicals, inflammatory responses and leukocyte recruitment, increases in cytokine production, edema formation, and other injuries of the microvascular structure (26). It is clinically important to accurately estimate individual's IP size for the selection of the optimal therapeutic strategy to salvage IP tissue while avoiding reperfusion injury.

In our study, we tried to create a CTP method to estimate the IP. We selected the relative values in relation to contralateral normal tissue. The main reason for doing so was to avoid uncertainty resulting from the differential hemodynamic characteristics between gray and white matter in part of the imaging parameters. The individual differences in brain tissue perfusion between the two hemispheres are another reason for using the relative values.

CBF, CBV, or MTT have been used to represent the hemodynamics of the ischemia region. Lee et al (27) reported that abnormalities on CBF and CBV maps can be challenging because of the physiological differences between gray and white matter. In contrast, the differences on MTT maps are minimal, making it more straightforward to depict regions with perfusion deficiency. Therefore, many studies (28,29) relied on MTT maps for the determination of perfusion defects. In our study, the abnormal regions on CBV and CBF maps enlarged progressively before 15–20 hours, but the regions with altered MTT or rMTT did not change obviously. So we proposed that the MTT map could sensitively reflect the hemodynamic changes, including infarct core, IP, and peripheral oligemia regions, but could not differentiate them.

Our IP thresholds were rCBF >0.203, rCBV >0.483. Because the sensitivity and specificity of rCBF threshold were higher than those of rCBV threshold, we used rCBF threshold to calculate the IP size. We compared the differences

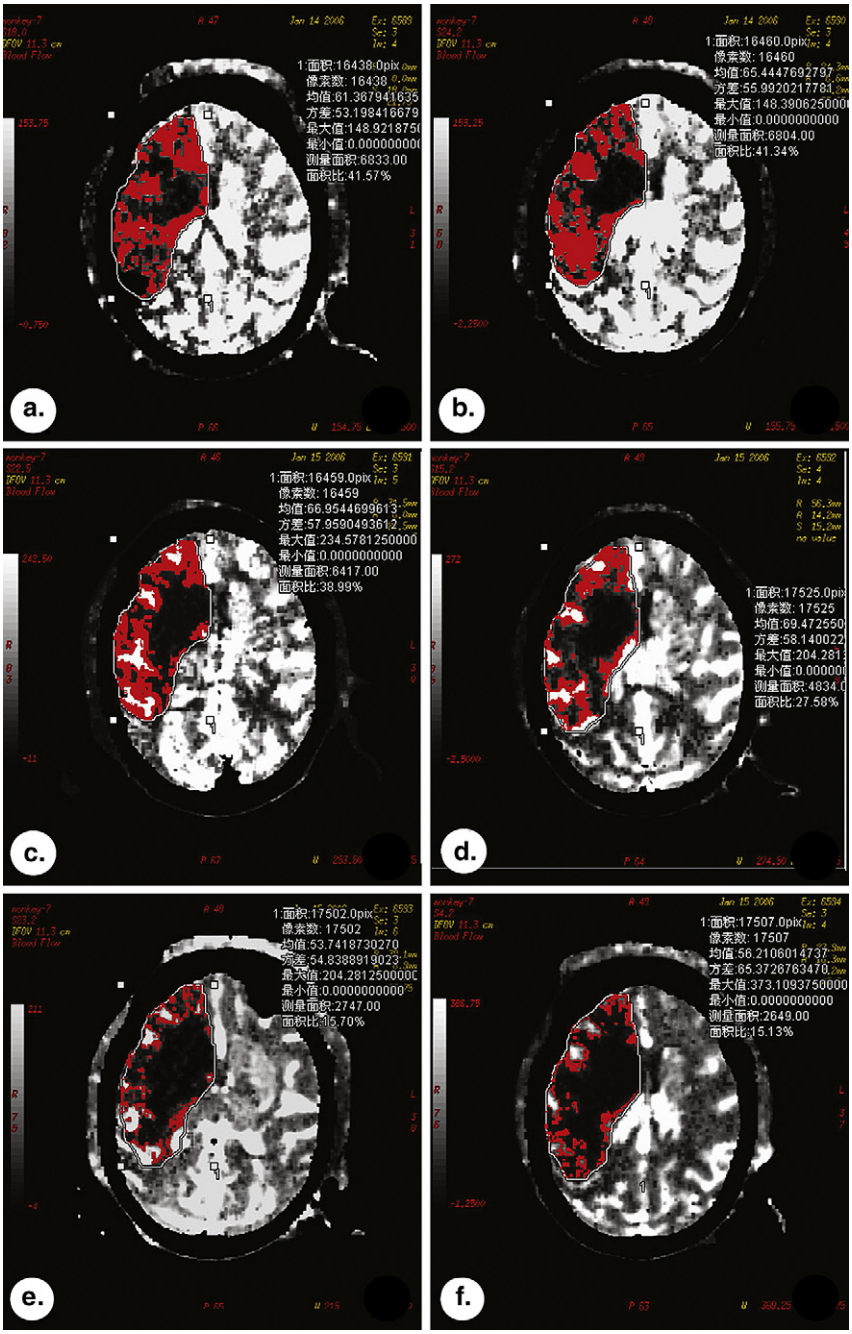

Figure 3. Dynamic evolution of size of ischemic penumbra (IP) measured by computed tomography perfusion method. **(a)** 1 hours; **(b)** 5 hours; **(c)** 10 hours; **(d)** 15 hours; **(e)** 20 hours; **(f)** 24 hours. The final infarct size marked by white curve was identified by T_2-weighted imaging at 24 hours. Red regions are pixels with relative cerebral blood flow value higher than the threshold (ie, IP). IP is located in the infarct margin. The size of IP reduced progressively.

between two methods in measuring the IP size. The IP size, as measured by MRI method, was larger than that of rCBF IP threshold before 15 hours, and lower at 20 and 24 hours. Therefore, the perfusion-diffusion mismatch region underestimated the exact IP in the early stage of ischemia, because in the early stage of ischemia, partial IP was present in the high signal intensity region on the DWI. At 20 and 24 hours, the abnormal regions of the CBF and MTT maps were larger than that of the CBV map, suggesting this mismatch region probably represented benign oligemia. Therefore, we concluded that MRI method could not represent IP exactly so the CTP method could display the evolution of IP more exactly than MRI method.

PS could reflect the integrality of blood-brain barrier (BBB) of ischemic region, which is important to thrombolysis therapy as hemorrhagic transformation (HT) of reperfused ischemic tissue would destroy the BBB and increase mortality (30,31). Bisdas et al (32) found in infarction patients with HT even without thrombolysis, PS in the ischemic voxels showed significantly higher than in the contralateral healthy tissue. In our study, there was no hemorrhage on noncontrast CT within 24 hours after MCAO. We found PS increased in ischemic region because of the reperfusion and BBB injury. And there were statistical differences among ROIs 1, 2, and 3 at 5 and 10 hours, suggesting that the intact of BBB and reperfusion or collateral blood flow were variable between infarct core and IP.

TABLE 4. IP Size (the Ratio to Infarct Size) in Monkey MCAO Model Calculated by Two Methods

Time points (hours)	Method	No. 1	No. 2	No. 3	No. 4	No. 5	$\bar{x} \pm s$
1	MRI	0.279	0.316	0.206	0.149	0.157	0.221 ± 0.074
	CTP	0.286	0.372	0.298	0.257	0.224	0.287 ± 0.055
5	MRI	0.225	0.214	0.183	0.163	0.137	0.184 ± 0.036
	CTP	0.267	0.298	0.277	0.24	0.201	0.257 ± 0.037
10	MRI	0.206	0.233	0.181	0.131	0.152	0.181 ± 0.041
	CTP	0.253	0.284	0.257	0.231	0.21	0.247 ± 0.028
15	MRI	0.181	0.156	0.169	0.125	0.123	0.151 ± 0.026
	CTP	0.216	0.201	0.203	0.175	0.175	0.194 ± 0.018
20	MRI	0.167	0.172	0.168	0.121	0.121	0.150 ± 0.026
	CTP	0.147	0.154	0.113	0.098	0.093	0.121 ± 0.028
24	MRI	0.076	0.089	0.124	0.056	0.115	0.092 ± 0.028
	CTP	0.051	0.076	0.107	0.068	0.087	0.078 ± 0.021

CTP, computerized tomography perfusion; IP, ischemic penumbra; MCAO, middle cerebral artery occlusion; MRI, magnetic resonance imaging.

MRI method represents perfusion-diffusion mismatch region.

Meanwhile, our method also had some limitations. First, our IP thresholds were calculated by monkey MCAO model, which may have some differences with human beings. Previous studies reported differential IP threshold of CBF or rCBF in different stroke populations. Astrup et al (1) confirmed that it demonstrated abnormal curves on electroencephalogram if the mean blood flow in the brain decreased to 20 mL/100 g/minute. It became a flat curve if it decreased to 15 mL/100 g/minute, the so-called electrophysiological function failure threshold. The Na-K pump and energy metabolism would fail if the blood flow decreased to 10 mL/100 g/minute, the so-called membrane function failure threshold. If the CBF was between these two function failure thresholds, the ischemic cells were reversible (ie, IP). If CBF was lower than the membrane function failure threshold, it evolved to infarction. Most authors (33–35) reported a variable membrane function failure threshold, ranged from 20 to 50 mL/100 g/minute. IP was never present if the CBF was lower than 6–15 mL/100 g/minute. Schaefer et al (32) reported that rCBF was the most effective parameter. Brain tissue with an rCBF value lower than 0.36 would not be IP, whereas those with an rCBF value larger than 0.79 would not be necrotic tissue. Neither rCBV nor MTT could distinguish IP from necrosis. However, it was clear that brain tissue with rCBV lower than 0.53 must be necrosis from follow-up examination results.

Second, the IP threshold was not absolute; it could vary by time of attack, circulation changes, individual difference, treatment, and other factors. The time window of IP in posterior circulation was much longer than in middle cerebral artery. The relative long interval between the first two time points is also a limitation of our study. The reason is that delayed excretion of high dose CT contrast would affect the results of CTP in short interval. Moreover, the accumulation of CT contrast in short time would aggravate the burden of heart function of monkeys. And at last, our IP sizes were calculated based on 24-hour T2WI. So the IP had not been salvaged, whereas the salvaged IP outside the abnormal signal intensity on T2WI was excluded. Thus our method could not identify whether the IP could be salvaged. Further studies could be focus on determining the exact IP quantities, and its relation between the IP size and the clinical therapy time window. The therapy time window of IP was crucial to thrombolysis therapy.

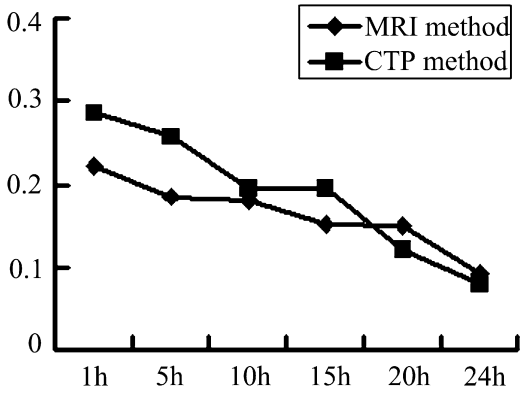

Figure 4. Comparison of the evolution of ischemic penumbra (IP) sizes estimated by two methods. IP decreases with time; before 15 hours, IP size by CTP method was larger than that by MRI method and lower at 20 hours and 24 hours. CTP, computed tomography perfusion; MRI, magnetic resonance imaging.

ACKNOWLEDGMENT

We express thanks to Dr. Wesley E. Daniels for correcting language errors.

REFERENCES

1. Astrup J, Siesjo BK, Symon L. Thresholds in cerebral ischemia – the ischemic penumbra. Stroke 1981; 12:723–725.
2. Hossmann KA. Viability thresholds and the penumbra of focal ischemia. Ann Neurol 1994; 36:557–565.

3. Ginsberg MD. Adventures in the pathophysiology of brain ischemia: penumbra, gene expression, neuroprotection: the 2002 Thomas Willis Lecture. Stroke 2003; 34:214–223.
4. Frykholm P, Anderssonj LR, Valtyssonj, et al. Ametabolic threshold of irreversible ischemia demonstrated by PET in a middle cerebral artery occlusion reperfusion primate model. Acta Eur Scand 2000; 102:18–26.
5. Takasawa M, Beech JS, Fryer TD, et al. Imaging of brain hypoxia in permanent and temporary middle cerebral artery occlusion in the rat using 18F-fluoromisonidazole and positron emission tomography: a pilot study. J Cereb Blood Flow Metab 2007; 27:679–689.
6. Wintermark M, Albers GW, Alexandrov AV, et al. Acute stroke imaging research roadmap. Stroke 2008; 39:1621–1628.
7. Akazawa K, Yamada K, Matsushima S, et al. Is it possible to define salvageable ischemic penumbra using semiquantitative rCBF levels derived from MR perfusion-weighted imaging? Neuroradiology 2008; 50:939–945.
8. Chavez JC, Zaleska MM, Wang X, et al. Multimodal magnetic resonance imaging for assessing evolution of ischemic penumbra: a key translational medicine strategy to manage the risk of developing novel therapies for acute ischemic stroke. J Cerebral Blood Flow Metab 2009; 29:217–219.
9. Desmond PM, Lovell AC, Rawlinson AA, et al. The value of apparent diffusion coefficient maps in early cerebral ischemia. AJNR Am J Neuroradiol 2001; 22:1260–1267.
10. Liu KF, Li F, Tatlisumak T, et al. Regional variations in the apparent diffusion coefficient and the intracellular distribution of water in rat brain during acute focal ischemia. Stroke 2001; 32:1897–1905.
11. Rosso C, Hevia-Montiel N, Deltour S, et al. Prediction of infarct growth based on apparent diffusion coefficients: penumbral assessment without intravenous contrast material. Radiology 2009; 250:184–192.
12. Loh PS, Butcher KS, Parsons MW, et al. Apparent diffusion coefficient thresholds do not predict the response to acute stroke thrombolysis. Stroke 2005; 36:2626–2631.
13. Lansberg MG, Thijs VN, Bammer R, et al. The MRA-DWI mismatch identifies patients with stroke who are likely to benefit from reperfusion. Stroke 2008; 39:2491–2496.
14. Schlaug G, Benfield A, Baird AE, et al. The ischemic penumbra: operationally defined by diffusion and perfusion MRI. Neurology 1999; 53: 1528–1537.
15. Muir KW, Baird-Gunning J, Walker L, et al. Can the ischemic penumbra be identified on noncontrast CT of acute stroke? Stroke 2007; 38:2485–2490.
16. Parsons MW, Pepper EM, Bateman GA, et al. Identification of the penumbra and infarct core on hyperacute noncontrast and perfusion CT. Neurology 2007; 68:730–736.
17. Soares BP, Dankbaar JW, Bredno J, et al. Automated versus manual post-processing of perfusion-CT data in patients with acute cerebral ischemia: influence on interobserver variability. Neuroradiology 2009; 51:445–451.
18. Tan JC, Dillon WP, Liu S, et al. Systematic comparison of perfusion-CT and CT-angiography in acute stroke patients. Ann Neurol 2007; 61:533–543.
19. Wintermark M, Flanders AE, Velthuis B, et al. Perfusion-CT assessment of infarct core and penumbra: receiver operating characteristic curve analysis in 130 patients suspected of acute hemispheric stroke. Stroke 2006; 37:979–985.
20. Hakim AM. Ischemic penumbra—the therapeutic window. Neurology 1998; 51(3 Suppl 3):S44–S46.
21. Warach S, Latour LL. Evidence of reperfusion injury, exacerbated by thrombolytic therapy, in human focal brain ischemia using a novel imaging marker of early blood-brain barrier disruption. Stroke 2004; 11:2659–2661.
22. Ebinger M, De Silva DA, Christensen S, et al. Imaging the penumbra – strategies to detect tissue at risk after ischemic stroke. J Clin Neurosci 2009; 16:178–187.
23. Hacke W, Kaste M, Bluhmki E, et al. Thrombolysis with alteplase 3 to 4.5 hours after acute ischemic stroke. N Engl J Med 2008; 359:1317–1329.
24. Kidwell CS, Alger JR, Saver JL. Evolving paradigms in neuroimaging of the ischemic penumbra. Stroke 2004; 35:2662–2665.
25. Darby DG, Barber PA, Gerraty RP, et al. Pathophysiological topography of acute ischemia by combined diffusion-weighted and perfusion MRI. Stroke 1999; 30:2043–2052.
26. Moore-Olufemi SD, Kozar RA, Moore FA, et al. Ischemia preconditioning protects against gut dysfunction and mucosal injury after ischemia/reperfusion injury. Shock 2005; 23:258–263.
27. Lee YZ, Lee JM, Vo K, et al. Rapid perfusion abnormality estimation in acute stroke with temporal correlation analysis. Stroke 2003; 34: 1686–1692.
28. Barber PA, Davis SM, Darb DG, et al. Absent middle cerebral artery flow predicts the presence and evolution of the ischemic penumbra. Neurology 1999; 52:1125–1132.
29. Rohl L, Ostergaard L, Simonsen CZ, et al. Viability thresholds of ischemic penumbra of hyperacute stroke defined by perfusion-weighted MRI and apparent diffusion coefficient. Stroke 2001; 32:1140–1146.
30. Aviv RI, d'Esterre CD, Murphy BD, et al. Hemorrhagic transformation of ischemic stroke: prediction with CT perfusion. Radiology 2009; 250: 867–877.
31. Huynh TJ, Murphy B, Pettersen JA, et al. CT perfusion quantification of small-vessel ischemic severity. AJNR Am J Neuroradiol 2008; 29: 1831–1836.
32. Bisdas S, Hartel M, Cheong LH, et al. Prediction of subsequent hemorrhage in acute ischemic stroke using permeability CT imaging and a distributed parameter tracer kinetic model. J Neuroradiol 2007; 34:101–108.
33. Heiss WD. Ischemic penumbra: evidence from functional imaging in man. J Cereb Blood Flow Metab 2000; 20:1276–1293.
34. Wintermark M, Fischbein NJ, Smith WS, et al. Accuracy of dynamic perfusion CT with deconvolution in detecting acute hemispheric stroke. AJNR Am J Neuroradiol 2005; 26:104–112.
35. Schaefer P, Ozsunar Y, He J, et al. Assessing tissue viability with MR diffusion and perfusion imaging. AJNR Am J Neuroradiol 2003; 24:436–443.